Models of the Manganese Catalase Enzymes. Dinuclear Manganese(III) Complexes with the $[Mn_2(\mu\text{-}O)(\mu\text{-}O_2CR)_2]^{2+}$ Core and Terminal Monodentate Ligands: Preparation and Properties of $[Mn_2O(O_2CR)_2X_2(bpy)_2]$ (X = Cl^-, N_3^-, H_2O)

John B. Vincent,[1a] Hui-Lien Tsai,[1b] Allan G. Blackman,[1a] Sheyi Wang,[1a] Peter D. W. Boyd,[1c] Kirsten Folting,[1d] John C. Huffman,[1d] Emil B. Lobkovsky,[1d] David N. Hendrickson,*[,1b] and George Christou*[,1a]

Contribution from the Department of Chemistry and the Molecular Structure Center, Indiana University, Bloomington, Indiana 47405-4001, and Department of Chemistry, 0506, University of California at San Diego, La Jolla, California 92093-0506

Received May 17, 1993®

Abstract: Procedures are reported that allow access to dinuclear Mn^{III} complexes possessing the $[Mn_2O(\mu\text{-}O_2CR)_2]^{2+}$ core. The complexes have the general formulation $[Mn_2O(O_2CR)_2X_2(bpy)_2]$ (X = Cl^-, N_3^-, H_2O; bpy = 2,2′-bipyridine) and are potential models of the Mn catalase enzymes. Treatment of $MnCl_2$/bpy/acetic acid reaction mixtures in MeCN with $NBu^n_4MnO_4$ in MeCN leads to subsequent isolation of $[Mn_2O(OAc)_2Cl_2(bpy)_2]\cdot AcOH\cdot H_2O$ (**1**). Analogous reactions allow the preparation of $[Mn_2O(O_2CPh)_2Cl_2(bpy)_2]\cdot 2H_2O$ (**2**) and $[Mn_2O(O_2CEt)_2Cl_2(bpy)_2]\cdot 3EtCO_2H\cdot H_2O$ (**3**). In the presence of N_3^-, the complex $[Mn_2O(O_2CPh)_2(N_3)_2(bpy)_2]$ (**5**) is obtained; use of AcO^- and a greater MnO_4^- amount yields $[Mn_2O_2(N_3)_4(bpy)_2]$ (**6**). Complex **1** can also be prepared from a reaction in which a solution of Cl_2 in MeCN is employed as the oxidizing agent instead of $NBu^n_4MnO_4$. If, however, aqueous HOAc is employed as the reaction medium, oxidation with an excess of Cl_2 leads to $[Mn_2O(OAc)_2(H_2O)_2(bpy)_2](ClO_4)_2$ (**7**). The three Mn_2 units are extremely similar and differ only in the identity of the terminal ligands X (Cl^-, N_3^-, or H_2O). They each contain a triply-bridged $[Mn_2(\mu\text{-}O)(\mu\text{-}O_2CR)_2]^{2+}$ core with chelating bpy and terminal X groups completing near-octahedral geometry at each Mn atom. In each case, the X group and an oxygen atom from a bridging RCO_2^- group lie on a Jahn–Teller elongation axis (high-spin d^4 Mn^{III}). Complexes **1**, **2**, **3**, and **5** have been studied by cyclic voltammetry in DMF; they each display a quasi-reversible oxidation at ~0.4 V (**1**, **2**, and **3**) and 0.18 V (**5**) *vs* ferrocene, assigned to the $2Mn^{III}/Mn^{III}Mn^{IV}$ couple. Variable-temperature solid-state magnetic susceptibilities of **1** and **5** were measured in the temperature range 5.0 to *ca.* 330 K. The effective magnetic moment per Mn_2^{III} (μ_{eff}) for **1** decreases gradually from 6.33 μ_B at 327.7 K to 5.85 μ_B at 100 K and then more steeply to 2.09 μ_B at 5.0 K. For **5**, μ_{eff} increases steadily from 6.96 μ_B at 320 K to a maximum of 8.12 μ_B at 30 K and then decreases to 7.45 μ_B at 5.0 K. The data were fit to a model that included an isotropic Heisenberg exchange interaction, an isotropic Zeeman interaction, and axial zero-field splitting terms for both ions. For complex **1**, a good fit was found with $J = -4.1$ cm^{-1}, $g = 1.88$, $D_1 = D_2 = -0.07$ cm^{-1}, and 0.8% by weight of a paramagnetic $S = 2$ impurity. For complex **5**, the corresponding values are $J = +8.8$ cm^{-1}, $g = 1.86$ and $D_1 = D_2 = 0.3$ cm^{-1}; the quality of the fit is less than that for **1**, and this was concluded to be due to the presence of *inter*molecular exchange interactions propagated by the intermolecular hydrogen-bonding network observed in the crystal structure of $5\cdot MeCN\cdot 4H_2O$. Thus, **5** is ferromagnetically coupled and has an $S = 4$ ground state. The J values for all available complexes containing the $[Mn_2O(O_2CR)_2]^{2+}$ core are compared, and a rationalization is suggested for the differences between **1**/**7** (negative J) and **5** (positive J). The relevance of these results to Mn catalase are discussed as well as to the observed difference in sign of the J values for deoxyhemerythrin (negative J) *versus* deoxy-N_3^--hemerythrin (positive J).

Introduction

It is now well established that a number of Mn-containing metalloenzymes contain tightly-bound Mn ions that are involved in the enzyme function.[2] These include certain bacterial superoxide dismutases, catalases, and ribonucleotide reductases and the photosynthetic water oxidation center of green plants and cyanobacteria.[2] Of particular relevance to this work are the catalases[2,3] and ribonucleotide reductase[2,4] whose study is still in its infancy, but which appear to possess a dinuclear Mn_2 site, as confirmed by preliminary X-ray crystallographic studies on the *Thermus thermophilus* enzyme.[3f] These complement detailed studies by other techniques that are strongly indicative of dinuclear sites.[3,5] On the basis of spectroscopic evidence, the manganese is thought to occur in a $[Mn_2(\mu\text{-}O)(\mu\text{-}O_2CR)_2]^{2+}$ core with N-based (histidine imidazole) peripheral ligands; evidence for the latter is beginning to appear.[6] As a result, a number of groups initially reported the preparation and characterization of Mn^{III}

• Abstract published in *Advance ACS Abstracts*, December 1, 1993.

(1) (a) Indiana University, Chemistry Department. (b) University of California at San Diego. (c) On leave from the University of Auckland, Auckland, New Zealand. (d) Indiana University Molecular Structure Center.

(2) Manganese Redox Enzymes; Pecoraro, V. L., Ed.; VCH: Weinheim, 1992.

(3) (a) Kono, Y.; Fridovich, I. *J. Biol. Chem.* **1983**, *258*, 13 646. (b) Kono, Y.; Fridovich, I. *J. Biol. Chem.* **1983**, *258*, 6015. (c) Beyer, W. F.; Fridovich, I. *Biochemistry* **1985**, *24*, 6460. (d) Barynin, V. V.; Grebenko, A. I. *Dokl. Akad. Nauk. SSSR* **1986**, *286*, 461. (e) Khangulov, S. V.; Barynin, V. V.; Melik-Adamyan, V. R.; Grebenko, A. I.; Voevodskaya, N. V.; Blyumenfeld, L. A.; Dobryakov, S. N.; Iiyasova, V. B. *Bioorg. Khim.* **1986**, *12*, 741. (f) Barynin, V. V.; Vagin, A. A.; Melik-Adamyan, V. R.; Grebenko, A. I.; Khangulov, S. V.; Popov, A. N.; Andrianova, M. E.; Vainshtein, B. K. *Dokl. Akad. Nauk. SSSR* **1986**, *288*, 877. (g) Khangulov, S. V.; Barynin, V. V.; Antonyuk-Barynina, S. V. *Biochim. Biophys. Acta* **1990**, *1020*, 25.

(4) Que, L., Jr.; True, A. E. *Prog. Inorg. Chem.* **1990**, *38*, 97, and references therein.

(5) (a) Fronko, R. M.; Penner-Hahn, J. E. *J. Am. Chem. Soc.* **1988**, *110*, 7554. (b) Waldo, G. S.; Fronko, R. M.; Penner-Hahn, J. E. *Biochemistry* **1991**, *30*, 10 486. (c) Waldo, G. S.; Yu, S.; Penner-Hahn, J. E. *J. Am. Chem. Soc.* **1992**, *114*, 5869.

(6) Dikanov, S. A.; Tsuetkov, Y. D.; Khangulov, S. V.; Goldfield, M. G. *Dokl. Akad. Nauk. SSSR* **1988**, *302*, 1255.

0002-7863/93/1515-12353$04.00/0

complexes with the $[Mn_2O(O_2CR)_2]^{2+}$ core and two tridentate N-based ligands capping each end of the molecule.[7,8] These modeling studies employing tridentate ligands have been important in establishing the accessibility of the $[Mn_2O(O_2CR)_2]^{2+}$ unit within synthetic complexes, but by blocking all three terminal coordination sites at each manganese, they preclude investigation of substrate or substrate–analogue binding studies. It was the goal of this study to prepare similarly bridged dinuclear complexes employing the bidentate ligand 2,2′-bipyridine (bpy), thus leaving a coordination site available for binding additional ligands; this strategy has already proven successful in Fe^{III} chemistry where bpy has allowed access to hemerythrin model complexes $[Fe_2O(OAc)_2Cl_2(bpy)_2]$ and $[Fe_2O(O_2CPh)_2(N_3)_2(bpy)_2]$[9] and, subsequently,[10] $[Fe_2O(mpdp)Cl_2(4,4'\text{-}Me_2bpy)]$ ($mpdpH_2$ = *m*-phenylenedipropionic acid). A preliminary communication[11] has reported our subsequent success in preparing $[Mn_2O(OAc)_2Cl_2(bpy)_2]$ and $[Mn_2O(O_2CPh)_2(N_3)_2(bpy)_2]$; at about the same time, Girerd and co-workers reported[12] the preparation of $[Mn_2O(OAc)_2(H_2O)_2(bpy)_2](PF_6)_2$.

We herein describe a variety of synthetic procedures that have allowed access to these complexes, including a high yield procedure to Girerd's bis-aquo cation, together with their structural characterization. This trio of complexes represents a great opportunity to investigate systematically the influence of the $Cl^-/N_3^-/H_2O$ groups on the structural and magnetic properties of the $[Mn_2O(O_2CR)_2]^{2+}$ core.

Experimental Section

Compound Preparation. All chemicals and solvents were used as received; all preparations were performed under aerobic conditions. $NBu^n_4MnO_4$ was prepared as described elsewhere.[13] Solutions of Cl_2 in MeCN were prepared by bubbling a calculated mass of Cl_2 into MeCN in a 100-mL volumetric flask and making up to the mark with MeCN. The resulting solution was standardized iodometrically and stored in a refrigerator. **WARNING: There have been reports of the detonation of quaternary ammonium permanganates during drying at elevated temperatures, and appropriate care should be taken; see ref 13a for more detail.**

$[Mn_2O(OAc)_2Cl_2(bpy)_2]\cdot AcOH\cdot H_2O$ (1). Method A. To a stirred solution of $MnCl_2\cdot 4H_2O$ (1.61 g, 8.14 mmol) and bpy (2.00 g, 12.8 mmol) in MeCN (30 mL) and acetic acid (6 mL) was added solid $NBu^n_4MnO_4$ (1.95 g, 5.40 mmol) in small portions. The resulting dark brown solution was filtered, and the filtrate was allowed to concentrate by evaporation. The well-formed black crystals were collected by filtration, washed with MeCN and Et_2O, and dried in air: yield 20–30%, based on total available Mn; electronic spectrum in CH_2Cl_2 λ_{max}, nm (ϵ_M/Mn, $L\cdot mol^{-1}\ cm^{-1}$) 492 (361), 556 (246); selected IR data (Nujol) 3350 (br, s), 1720 (s), 1600 (s), 1580 (s), 1335 (m), 1310 (m), 1245 (m), 1150 (m), 1055 (m), 1035 (m), 775 (s), 725 (s), 655 (s), 600 (m). Anal. Calcd for $C_{26}H_{28}N_4O_8Cl_2Mn_2$: C, 44.28; H, 4.00; N, 7.94; Cl, 10.05; Mn, 15.58. Found: C, 43.4; H, 3.9; N, 7.7; Cl, 10.05; Mn, 15.4.

Method B. To a stirred solution of $Mn(OAc)_2\cdot 4H_2O$ (2.00 g, 8.16 mmol), bpy (2.00 g, 12.8 mmol), and $NEt_4Cl\cdot H_2O$ (3.0 g, 20 mmol) in MeCN (30 mL) and acetic acid (6 mL) was added solid $NBu^n_4MnO_4$ (1.95 g, 5.40 mmol) in small portions. The resulting dark brown solution was worked up as in method A, and the identity of obtained complex **1** was confirmed by electronic and IR spectral comparison.

Method C. To a warm solution of $Mn(OAc)_2\cdot 4H_2O$ (2.00 g, 8.16 mmol) and bpy (1.27 g, 8.13 mmol) in MeCN/HOAc (20 mL/6 mL) was added Cl_2 in MeCN (0.99 M, 4.10 mL, 4.06 mmol). The flask was immediately stoppered and the dark orange-brown solution was stirred for 40 min at room temperature. The solution was filtered to remove a pale precipitate, and the filtrate was left undisturbed for 3 days in a stoppered flask at room temperature. The resulting black crystals were collected by filtration, washed with ice-cold MeCN (2 × 3 mL), and air dried. The yield was 1.05 g (41%). The product was characterized by comparison of its IR spectrum with that of authentic material.

$[Mn_2O(O_2CPh)_2Cl_2(bpy)_2]\cdot 2H_2O$ (2). Method A. To a stirred solution/slurry of $MnCl_2\cdot 4H_2O$ (1.61 g, 8.1 mmol), bpy (2.00 g, 12.8 mmol), and benzoic acid (5.0 g, 41 mmol) in MeCN (30 mL) was added solid $NBu^n_4MnO_4$ (1.95 g, 5.40 mmol) in small portions. The resulting homogeneous, dark brown solution was slowly concentrated by evaporation, and the dark red crystalline precipitate was collected by filtration, washed with a little MeCN and Et_2O, and dried in air: yield ~10%. The identity of the product was confirmed by crystallography and by electronic and spectral comparison with material obtained as described below.

Method B. To a slurry of complex **1** (0.35 g, 0.50 mmol) in CH_2Cl_2 (30 mL) was added solid benzoic acid (0.25 g, 2.0 mmol). The resulting brown solution soon began to precipitate dark red microcrystals, and, after 2 h, they were collected by filtration, washed with Et_2O, and dried in air: yield ~95%; electronic spectrum in DMF 280 (1.5 × 10^4), 340 (sh, 740), 502 (sh, 135); IR data (Nujol) 3400 (br, s), 1595 (s), 1555 (s), 1310 (m), 1250 (m), 1165 (m), 1155 (m), 1100 (m), 1075 (m), 1030 (s), 765 (s), 720 (vs), 655 (m). Anal. Calcd for $C_{34}H_{30}N_4O_7Cl_2Mn_2$: C, 51.86; H, 3.84; N, 7.12; Cl, 9.00. Found: C, 50.9; H, 3.9; N, 7.1; Cl, 9.3.

$[Mn_2O(O_2CEt)_2Cl_2(bpy)_2]\cdot 3EtCO_2H\cdot H_2O$ (3). To a stirred slurry of $MnCl_2\cdot 4H_2O$ (1.61 g, 8.14 mmol) and bpy (2.00 g, 12.8 mmol) in MeCN (30 mL) and propionic acid (6 mL) was added solid $NBu^n_4MnO_4$ (1.95 g, 5.40 mmol) in small portions. The resulting homogeneous, dark brown solution was filtered and left undisturbed at ambient temperature for several hours. The black crystals were collected by filtration, washed with Et_2O, and dried in air: yield ~20%; electronic spectrum in DMF 283 (7 × 10^3), 468 (sh, 275); IR data (Nujol) 3400 (br, s), 1730 (s), 1600 (s), 1580 (s), 1310 (m), 1250 (m), 1170 (m), 1100 (m), 1070 (m), 1030 (m), 870 (s), 830 (s), 650 (m), 590 (m). Anal. Calcd for $C_{35}H_{46}N_4O_{12}Cl_2Mn_2$: C, 46.94; H, 5.18; N, 6.26; Cl, 7.92; Mn, 12.27. Found: C, 46.6; H, 5.1; N, 6.3; Cl, 8.12; Mn, 12.4.

$[Mn_4O_2(OAc)_7(bpy)_2](Br_3)\cdot H_2O$ (4). To a stirred slurry of $MnBr_2\cdot 4H_2O$ (2.33 g, 8.12 mmol) and bpy (2.00 g, 12.8 mmol) in MeCN (30 mL) and acetic acid (6 mL) was added solid $NBu^n_4MnO_4$ (1.95 g, 5.4 mmol) in small portions. The resulting brown solution was filtered, and the filtrate was allowed to concentrate by evaporation to give red-brown crystals. These were collected by filtration, washed with a little MeCN, and dried in air: yield ~60%. Anal. Calcd for $C_{34}H_{39}N_4O_{17}Br_3Mn_4$: C, 33.06; H, 3.18; N, 4.54; Br, 19.41; Mn, 17.79. Found: C, 33.2; H, 3.25; N, 4.5; Br, 19.9; Mn, 18.0.

$[Mn_2O(O_2CPh)_2(N_3)_2(bpy)_2]$ (5). Method A. To a solution of $Mn(O_2CPh)_2\cdot 2H_2O$ (2.57 g, 8.14 mmol) and NEt_4N_3 in MeCN (45 mL) were added $PhCO_2H$ (4.00 g, 32.8 mmol) and bpy (1.63 g, 10.4 mmol) in that order. Solid $NBu^n_4MnO_4$ (0.82 g, 2.27 mmol) was then added in small portions with stirring to give a deep red-brown solution. After 5 min, the solution was filtered, and the filtrate was allowed to concentrate by evaporation to give a brown crystalline product. This was collected by filtration, washed with MeCN and Et_2O, and dried *in vacuo*: yield 45–63%; selected IR data (Nujol) 3450 (br), 2047 (vs), 1599 (s), 1556 (s), 1495 (m), 1446 (s), 1336 (m), 1313 (m), 1278 (m), 1250 (m), 1030 (s), 765 (s), 731 (s), 721 (s), 675 (m), 660 (m), 435 (m); electronic spectrum in DMF 280 (1.7 × 10^4), 416 (sh, 492). Anal. Calcd for $C_{35}H_{30.5}N_{10.5}O_{6.5}Mn_2$ (**5**·MeCN·3/2H_2O): C, 51.93; H, 3.87; N, 18.51. Found: C, 51.66; H, 3.57; N, 18.39.

The sample for crystallography was obtained from a separate preparation. The crystals were not dried *in vacuo*, and the crystallographic study established the formulation **5**·MeCN·$4H_2O$.

Method B. A slurry of $MnCl_2\cdot 4H_2O$ (1.61 g, 8.14 mmol) and NaN_3 (1.05 g, 16.3 mmol) in MeCN (45 mL) was stirred for 10 min, and then $PhCO_2H$ (4.00 g, 32.8 mmol) and bpy (1.63 g, 10.4 mmol) were added in that order to give a yellow slurry. Solid $NBu^n_4MnO_4$ (0.82 g, 2.27 mmol) was then slowly added in small portions with stirring to give a red-brown solution. This was filtered, and the filtrate was allowed to concentrate by evaporation to give dark brown crystals. These were collected by filtration, washed with MeCN and Et_2O, and dried *in vacuo*: yield 55–78%. Anal. Calcd for $C_{63.3}H_{30}N_{10}O_{6.67}Mn_2$ (**5**·H_2O·1/3$PhCO_2H$): C, 53.01; H, 3.67; N, 17.01. Found: C, 53.44; H, 3.68; N, 17.09.

(7) Sheats, J. E.; Czernuszewicz, R. S.; Dismukes, G. C.; Rheingold, A. L.; Petrouleas, V.; Stubbe, J.; Armstrong, W. H.; Beer, R. H.; Lippard, S. J. *J. Am. Chem. Soc.* **1987**, *109*, 1435.

(8) Wieghardt, K.; Bossek, U.; Ventur, D.; Weiss, J. *J. Chem. Soc., Chem. Commun.* **1985**, 347.

(9) Vincent, J. B.; Huffman, J. C.; Christou, G.; Li, Q.; Nanny, M. A.; Hendrickson, D. N.; Fong, R. H.; Fish, R. H. *J. Am. Chem. Soc.* **1988**, *110*, 6898.

(10) Beer, R. H.; Tolman, W. B.; Bott, S. G.; Lippard, S. J. *Inorg. Chem.* **1991**, *30*, 2082.

(11) Vincent, J. B.; Folting, K.; Huffman, J. C.; Christou, G. *Biochem. Soc. Trans.* **1988**, *16*, 822.

(12) Menage, S.; Girerd, J.-J.; Gleizes, A. *J. Chem. Soc., Chem. Commun.* **1988**, 431.

(13) (a) Vincent, J. B.; Chang, H.-R.; Folting, K.; Huffman, J. C.; Christou, G.; Hendrickson, D. N. *J. Am. Chem. Soc.* **1987**, *109*, 5703. (b) Kulawiec, R. J.; Crabtree, R. H.; Brudvig, G. W. *Inorg. Chem.* **1988**, *27*, 1309.

$[Mn_2O_2(N_3)_4(bpy)_2]$ (6). Solid $NBu^n_4MnO_4$ (1.95 g, 5.40 mmol) was added in small portions to a stirred, yellow slurry of $Mn(OAc)_2{\cdot}4H_2O$ (2.00 g, 8.16 mmol), bpy (2.00 g, 12.8 mmol), and NaN_3 (0.86 g, 13.2 mmol) in MeCN (30 mL) and acetic acid (6 mL). The resulting dark brown solution was filtered, and the filtrate was left at ambient temperature. After 1 h, the black microcrystalline precipitate was collected by filtration, washed with MeCN, and dried in air: yield ~30%. **CARE: On one occasion, a batch of larger crystals exploded on a frit during drying at ambient temperature:** selected IR data (Nujol) 2020 (vs, br), 1310 (m), 1275 (m), 1155 (m), 1100 (m), 1025 (s), 765 (s), 725 (s), 665 (s), 650 (m), 640 (m), 565 (s), 430 (s). Anal. Calcd for $C_{20}H_{16}N_{16}O_2Mn_2$: C, 38.60; H, 2.59; N, 36.01; Mn, 17.66. Found: C, 38.9; H, 2.8; N, 35.7; Mn, 16.8.

$[Mn_2O(OAc)_2(H_2O)_2(bpy)_2](ClO_4)_2$ (7). Method A. To a warm (~40 °C) yellow solution of $Mn(OAc)_2{\cdot}4H_2O$ (10.0 g, 40.8 mmol) and bpy (6.35 g, 40.7 mmol) in H_2O/HOAc (100 mL/30 mL) was added $NaClO_4$ (10.0 g, 82.0 mmol). Chlorine gas was bubbled through the yellow solution until a dark brown coloration was obtained. The solution was stirred while being maintained in an icebath for 1.5 h, and the resulting grey powder was collected by filtration, washed with ice-cold EtOH (2 × 5 mL) and Et_2O (2 × 5 cm^3), and air dried. The yield was 12.0 g (74%). Crystals suitable for crystallography were obtained by allowing the filtrate from a preparation on a smaller scale to remain undisturbed at room temperature for 24 h. Anal. Calcd for $C_{24}H_{26}N_4O_{15}Cl_2Mn_2$: C, 36.43; H, 3.31; N, 7.08; Cl, 8.96. Found: C, 36.0; H, 3.2; N, 6.7; Cl, 9.5.

Method B. To a warm yellow solution of $Mn(OAc)_2{\cdot}4H_2O$ (2.0 g, 8.2 mmol) and bpy (1.27 g, 8.13 mmol) in H_2O/HOAc (20 mL/6 mL) was added a solution of $NaIO_4$ (0.22 g, 1.03 mmol) in H_2O (5 mL). The yellow solution rapidly turned dark brown. To this solution was added $NaClO_4$ (2.0 g, 16 mmol), and the flask was placed in an ice bath. Subsequent steps were the same as for method A. The yield was 1.2 g (37%). The product was identified as **7** by IR spectral comparison with an authentic sample.

$[Mn_2O_2(OAc)Cl_2(bpy)_2]{\cdot}$EtOH (8). Complex **1** (0.10 g, 0.14 mmol) was dissolved in a minimum of distilled water (~5 mL). The flask was immediately placed on a vacuum line, and the solvent was removed under vacuum. The remaining brown solid was collected on a frit, washed with a little EtOH and Et_2O, and dried under vacuum: yield ~60%. The identity of the product was confirmed by electronic and IR spectral comparison with an authentic sample.[14] Anal. Calcd for $C_{23}H_{29}N_4O_8Cl_2Mn_2$: C, 41.21; H, 4.36; N, 8.36; Cl, 10.58; Mn, 16.39. Found: C, 41.3; H, 4.0; N, 7.7; Cl, 10.6; Mn, 16.8.

Conversion of 1 to $[Mn_4O_2(OAc)_7(bpy)_2](ClO_4){\cdot}3H_2O$. To a stirred slurry of complex **1** (0.35 g, 0.50 mmol) in MeCN (30 mL) was added NaOAc (0.080 g, 1.0 mmol) and HOAc (5 mL). After a few minutes, $NBu^n_4ClO_4$ (0.090 g, 0.25 mmol) was added, and the mixture was stirred for a further 60 mins. The resulting deep red solution was filtered. The filtrate deposited some additional white solid on standing and was therefore filtered again when precipitation ceased. The resulting filtrate was concentrated under vacuum to ~5 mL, and Et_2O was added dropwise until precipitation of a fine red precipitate was complete. The solid was collected by filtration, washed with EtOH and Et_2O, and dried in air. The product was identified as $[Mn_4O_2(OAc)_7(bpy)_2](ClO_4){\cdot}3H_2O$ by IR comparison with an authentic sample:[15] yield 56%.

X-ray Crystallography. Data were collected at −155, −146, and −155 °C for complexes **1**, **5**·MeCN·$4H_2O$, and **7**, respectively, on a Picker four-circle diffractometer. Details of the diffractometry, low-temperature facilities, and computational procedures employed by the Molecular Structure Center have been described elsewhere.[16] Pertinent parameters are listed in Table I. Structures were solved by the usual combination of direct methods (MULTAN) and Fourier techniques and refined by full-matrix least squares.

For complex **1**, a systematic search of a limited hemisphere of reciprocal space located a set of diffraction maxima with symmetry and systematic absences corresponding to the unique monoclinic space group $P2_1/n$. Subsequent solution and refinement of the structure confirmed this choice. All non-hydrogen atoms were successfully located and refined with anisotropic thermal parameters and with no sign of any disorder problems.

Table I. Crystallographic Data for Complexes **1**,**5**·MeCN·$4H_2O$, and **7**

	1	**5**	**7**
cryst system	monoclinic	monoclinic	monoclinic
space group	$P2_1/n$	$C2/c$	$C2/c$
temp, °C	−155	−146	−155
a, Å	16.897(12)[a]	16.232(7)[b]	33.939(18)[c]
b, Å	8.264(5)	26.240(14)	8.561(3)
c, Å	21.678(18)	9.535(4)	21.565(10)
β, deg	91.77(4)	101.95(2)	105.88(3)
Z	4	4	8
vol, Å^3	3025.36	3973.17	6026.60
abs coeff, cm^{-1}	10.307	6.572	10.552
scan speed, deg min^{-1}	4.0	4.0	4.0
total data	4300	4222	4442
unique data	3575	2615	3968
obsd data	1466[d]	1663[e]	3373[e]
$R(R_w)$, %	7.85 (7.57)	7.80 (7.52)	5.20 (5.37)

[a] Thirty-four reflections at −155 °C. [b] Thirty-two reflections at −146 °C. [c] Thirty-two reflections at −155 °C. [d] $F > 2.33\sigma(F)$. [e] $F > 3.00\sigma(F)$.

In subsequent stages, one molecule each of acetic acid and H_2O were located in the asymmetric unit. A difference Fourier at this stage revealed some hydrogen atoms, but no attempt to refine them was made; instead, hydrogen atoms were included as fixed-atom contributors, except for those of the solvent molecules which were omitted. The final difference map was essentially featureless. Final values of conventional indices R and R_w are included in Table I.

For complexes **5**·MeCN·$4H_2O$ and **7**, a systematic search of limited hemispheres of reciprocal space located sets of diffraction maxima that exhibited monoclinic symmetry. The systematic absences of hkl for $h + k = 2n + 1$ and $00l$ for $l = 2n + 1$ identified the space group as either C_2/c or Cc. The choice of the centrosymmetric space group C_2/c was confirmed by the successful solution and refinement of the structures. For complex **5**, the dinuclear unit lies on a crystallographic 2-fold axis passing through bridging oxygen atom O(23); the asymmetric unit thus contains half the molecule, together with two molecules of H_2O and half a molecule of CH_3CN, the methyl carbon of which lies on the 2-fold axis. All non-hydrogen atoms were readily located and refined with anisotropic thermal parameters except for the MeCN molecule which was refined isotropically. All hydrogen atoms were included in the latter stages as fixed-atom contributors except for those of the solvents, which were omitted. The final difference map was essentially featureless. Final values of R and R_w are included in Table I.

For complex **7**, the asymmetric unit contains the dinuclear unit and two ClO_4^- ions. All non-hydrogen atoms were readily located and refined anisotropically with no disorder problems being encountered; all hydrogen atoms were visible in a subsequent difference Fourier phased on the non-hydrogen atoms. The hydrogen atoms were included in the final cycles and refined isotropically. The hydrogen atoms of the water molecules were somewhat ill-behaved, exhibiting large thermal parameters, but their removal increased the discrepancy indices slightly, and the hydrogen atoms reappeared in subsequent difference Fourier maps, so they were reincluded. The final difference map was essentially featureless. Final values of R and R_w are included in Table I.

Physical Measurements. Variable-temperature DC magnetic susceptibility data were measured by using a Quantum Design MPMS SQUID susceptometer equipped with a 5.5 T magnet. The susceptometer was operated at a magnetic field strength of 10 kG. Diamagnetic corrections were estimated from Pascal's constants and subtracted from the experimental susceptibility data to obtain the molar paramagnetic susceptibilities of the compounds. These susceptibilities were fit to the appropriate theoretical expressions by means of a least-squares-fitting computer program.[17]

Results

Syntheses. Previous work had established $NBu^n_4MnO_4$ as a useful new reagent for the synthesis in *nonaqueous* media of Mn complexes in the oxidation state range II–IV and with various nuclearities.[13,15,18] The synthetic strategy is a comproportionation reaction between MnO_4^- and Mn^{II} in the presence of appropriate

(14) Bashkin, J. S.; Schake, A. R.; Vincent, J. B.; Chang, H.-R.; Li, Q.; Huffman, J. C.; Christou, G.; Hendrickson, D. N. *J. Chem. Soc., Chem. Commun.* **1988**, 700.

(15) Vincent, J. B.; Christmas, C.; Chang, H.-R.; Li, Q.; Boyd, P. D. W.; Huffman, J. C.; Hendrickson, D. N.; Christou, G. *J. Am. Chem. Soc.* **1989**, *111*, 2086.

(16) Chisholm, M. H.; Folting, K.; Huffman, J. C.; Kirkpatrick, C. C. *Inorg. Chem.* **1984**, *23*, 1021.

(17) Chandler, J. P. *QCPE* **1973**, 66.

(18) Vincent, J. B.; Huffman, J. C.; Christou, G. *Inorg. Chem.* **1986**, *25*, 996.

ligands and in MeCN, EtOH, or DMF (or combinations thereof) as reaction solvent. Of particular relevance to the present work was the observation[15] that $NBu^n_4MnO_4$, $Mn(OAc)_2$, $NBu^n_4ClO_4$, PhCOOH, and bpy in MeCN lead directly to high yields (~60%) of the tetranuclear complex $[Mn_4O_2(O_2CPh)_7(bpy)_2](ClO_4)$ originally prepared[15] by the reaction of bpy with preisolated $[Mn_3O(O_2CPh)_6(py)_3](ClO_4)$. In a subsequent experiment, it was discovered that the at-first-glance trivial replacement of $Mn(OAc)_2$ with $MnCl_2$ led to a completely different product. No sign of the red color of the tetranuclear complex was observed; instead, concentration of the brown reaction solution led to isolation of black crystals identified as complex **2**. Addition of a cosolvent was avoided as this causes precipitation of reaction byproducts, leading to messy mixtures difficult to purify. A more convenient procedure to **2** is ligand exchange with **1** (95% yield), as described below (*vide infra*). Subsequent extension of this method to acetic and propionic acids allowed access to the corresponding complexes **1** and **3**, respectively. Complex **1** was structurally characterized confirming the formulation $[Mn_2O(OAc)_2Cl_2(bpy)_2]\cdot AcOH\cdot H_2O$.

The $[Mn_2(\mu\text{-}O)(\mu\text{-}O_2CR)_2]$ unit in complexes **1–3** represents one-half of the $[Mn_4(\mu_3\text{-}O)_2(\mu\text{-}O_2CR)_4]$ core in the tetranuclear cation $[Mn_4O_2(O_2CR)_7(bpy)_2]^+$. The presence of the Cl^- ions provided by $MnCl_2$ can thus be considered as "trapping" the dinuclear fragment preventing dimerization to Mn_4O_2-containing products. We make no firm mechanistic implication by this statement, however, since there is no direct evidence that Mn_2O species are intermediate in the formation of the tetranuclear materials (*vide infra*). Note that complex **1** is also the product when $Mn(OAc)_2$ is used in the reaction in the presence of NEt_4Cl, so that **1** is not formed because of the absence of free AcO^- ions in the medium.

Extension of the above procedure to other halides has been explored. When the reaction was carried out using NBu^n_4F instead of NEt_4Cl, the presence of F^- appeared (visually) to also suppress formation of red $[Mn_4O_2(OAc)_7(bpy)_2]^+$, but it proved difficult to isolate and identify the product(s); black oils were repeatedly obtained that proved difficult to purify. With $MnBr_2$, a black crystalline precipitate was obtained that proved to be complex **4** in 60% isolated yield; i.e., the $[Mn_4O_2(OAc)_7(bpy)_2]^+$ moiety was now formed. The use of I^- was also unsuccessful; it is too good a reducing agent for higher oxidation state Mn and did not yield any higher oxidation state (>II) product. Overall, the use of Cl^- appears to be the optimum method for diverting the reaction to the dinuclear products and allowing their isolation in pure form.

The complex $[Mn_2O(OAc)_2(HB(pz)_3)_2]$, containing a similar $[Mn_2(\mu\text{-}O)(\mu\text{-}OAc)_2]^{2+}$ core as **1**, has been shown to undergo facile carboxylate exchange.[7] Complex **1** displays similar reactivity, as shown by its reaction with excess PhCOOH which converts it, essentially quantitatively (95% isolated yield), to **2**, as summarized in eq 1. No complicating side reactions involving the Mn–Cl bonds are thus occurring, as

$$[Mn_2O(OAc)_2Cl_2(bpy)_2] + 2PhCOOH \rightarrow [Mn_2O(O_2CPh)_2Cl_2(bpy)_2] + 2HOAc \quad (1)$$

had seemed a possibility. Similar carboxylate-exchange reactions have also been seen for $[Mn_4O_2(OAc)_7(bpy)_2]^+$ and $[Mn_4O_2(OAc)_7(pic)_2]^-$.[15,19]

At this point, we wondered whether similar dinuclear species could be isolated with "pseudohalide" monoanionic ligands. Azide was the ligand of choice because of its biological relevance, being an inhibitor of certain catalases.[2] The presence of N_3^- in a related reaction mixture led to isolation of complex **5**, the formulation of which as $[Mn_2O(O_2CPh)_2(N_3)_2(bpy)_2]$ was confirmed by crystallography. Interestingly, however, attempts to make the corresponding AcO^- complex instead yielded complex **6**, $Mn_2O_2(N_3)_4(bpy)_2$. Structural characterization of **6** was thwarted by the instability of larger crystals (explosively, on one occasion) although microcrystalline material is well behaved. In accord with the analytical composition, it seems reasonable that this is a Mn^{IV} dimer with two $\mu\text{-}O^{2-}$ groups and a bpy and two N_3^- ligands terminally coordinated to each Mn. There are now several examples of the $[Mn_2(\mu\text{-}O)_2]^{4+}$ core bound to exclusively N-based peripheral ligands.[4]

An additional reactivity characteristic established to date for complex **1** involves its behavior in aqueous solution. Dissolution of **1** in a minimum of water followed by immediate removal of solvent under vacuum yields a brown powder. This product was concluded to be the $Mn_2^{III,IV}$ complex **8**, $[Mn_2O_2(OAc)Cl_2(bpy)_2]$, based on analytical data and spectroscopic comparison with authentic material.[14] The effect of brief dissolution in water is thus the hydrolytically-induced formation of a higher oxidation state product, probably via disproportionation. Similar behavior under similar conditions has previously been reported[20] for $[Mn_2O(OAc)_2(TACN)_2]^{2+}$ (TACN = 1,4,7-triazacyclononane), which hydrolyzes in water to yield $[Mn_2O_2(OAc)(TACN)_2]^{2+}$. The ~60% yield of **8** is consistent with eq 2, the Mn^{II} byproduct being removed in the

$$3Mn_2^{III} \xrightarrow{H_2O} 2Mn_2^{III,IV} + 2Mn^{II} \quad (2)$$

wash. Again, the presence of Mn–Cl linkages in **1** does not provide complicating side reactions; all chemistry seems to be concentrated in the bridging region.

It was proposed above that the Cl^- possibly functions to "trap" the dinuclear $[Mn_2O]$ fragment, preventing its aggregation to a $[Mn_4O_2]$ product. If so, it seemed reasonable to suspect that, under appropriate conditions, preisolated **1** could be converted to a tetranuclear species. This has now been demonstrated. Treatment of **1** with acetic acid and NaOAc, the latter to help sequester Cl^- as NaCl, led to the characteristic red coloration of $[Mn_4O_2]^{8+}$ complexes; addition of ClO_4^- led to isolation of known[15] $[Mn_4O_2(OAc)_7(bpy)_2](ClO_4)\cdot 3H_2O$ in 56% yield. The conversion can be summarized in eq 3; the HOAc was essential for high yield conversion.

$$2[Mn_2O(OAc)_2Cl_2(bpy)_2] + 4NaOAc \xrightarrow{HOAc} [Mn_4O_2(OAc)_7(bpy)_2]^+ + 2bpy + AcO^- + 4\,NaCl \quad (3)$$

This transformation lends some support for the possibility that, in the absence of Cl^-, the synthetic procedure that leads directly to $[Mn_4O_2]^{8+}$ products from MnO_4^- and Mn^{II} reagents does proceed *via* the intermediacy of $[Mn_2O]^{4+}$ units. Attempts to effect the reverse reaction, i.e., cleavage of $[Mn_4O_2(OAc)_7(bpy)_2]^+$ with Cl^- and bpy to yield complex **1**, have proven unsuccessful.[21]

Syntheses Using Elemental Chlorine. It has been discovered that the $NBu^n_4MnO_4$ may be replaced with other oxidizing agents. Elemental Cl_2, dissolved in MeCN, has provided a preparative route (method C) to higher yields of complex **1** (~40%) than that available from the comproportionation procedures. Thus, addition of 0.5 equiv of Cl_2 to $Mn(OAc)_2\cdot 4H_2O$ and bpy in MeCN/HOAc yields the Mn^{III}_2 complex **1**, as expected from eq 4. Addition of only 0.25 equiv of Cl_2 leads to lower yields of **1**

$$2Mn^{II} + Cl_2 \rightarrow 2Mn^{III} + 2Cl^- \quad (4)$$

rather than a Mn^{II}, Mn^{III} product. If either 0.75 or 1.0 equiv of Cl_2 are used, the brown solution undergoes a further color change to dark green, characteristic of a Mn^{IV}-containing product, and an olive-green, sparingly-soluble powder is precipitated. The latter

(19) Libby, E.; McCusker, J. K.; Schmitt, E. A.; Folting, K.; Hendrickson, D. N.; Christou, G. *Inorg. Chem.* **1991**, *30*, 3486.

(20) Wieghardt, K.; Bossek, U.; Nuber, B.; Weiss, J.; Bonvoisin, J.; Corbella, M.; Vitols, S. E.; Girerd, J. J. *J. Am. Chem. Soc.* **1988**, *110*, 7398.

(21) In contrast to the behavior of the analogous Fe_4 complex, which is converted to an Fe_2 product, see ref 9.

appears similar but not identical to complex **8**. The low solubility of this product has hitherto foiled attempts at purification and/or crystallization.

In contrast to the results in MeCN/HOAc, parallel reactions in H_2O/HOAc have led to only Mn^{III} products, even in the presence of an excess of Cl_2. Thus, bubbling of Cl_2 through an aqueous HOAc solution of $Mn(OAc)_2{\cdot}4H_2O$ and bpy gives a dark brown solution from which may be isolated complex **7** in high yield (74%) on addition of $NaClO_4$. The cation has already been reported as the PF_6^- salt by Girerd and co-workers from a comproportionation reaction in aqueous MeOH.[12] The present procedure is particularly facile and high yield. Because of the low solubility of Cl_2 in H_2O, quantitative addition of aqueous Cl_2 solutions was not attempted; however, prolonged bubbling of Cl_2 through the reaction mixture gave the same product, **7**.

Other water-soluble oxidizing agents were also briefly explored. Addition of $^1/_8$ equiv of $NaIO_4$ to the aqueous HOAc solution of $Mn(OAc)_2{\cdot}4H_2O$/bpy rapidly led to a dark brown solution and isolation of **7** on addition of $NaClO_4$. Greater amounts of $NaIO_4$ led to mixtures of **7** and an unidentified red-brown solid. Similarly, addition of 1 equiv of $(NH_4)_2S_2O_8$ not only led to slower formation of a dark brown solution but also then gave **7** on addition of $NaClO_4$. If no $NaClO_4$, is added, slower formation of $[Mn_2O(OAc)_2(H_2O)(S_2O_8)(bpy)_2]$ crystals results; the latter contains a bound $S_2O_8^{2-}$ ligand and has been described elsewhere.[22]

Description of Structures. The structures of **1**, **5**, and the anion of **7** are shown in Figure 1, and important interatomic distances and angles are compared in Table II. For complex **1**, the two Mn atoms are bridged by two AcO^- and one O^{2-} groups across an intermetal separation of 3.153(3) Å. A Cl^- and a bpy group complete distorted octahedral geometry at each metal center. The molecule has nonimposed C_2 symmetry, and the Cl(3)–Mn(1)–Mn(2)–Cl(4) torsional angle is 81.6°. There is clear evidence for a Jahn–Teller elongation (high-spin d^4 Mn^{III}). The Mn–carboxylate distances fall into two statistically-inequivalent groups differing by over 0.2 Å, and the Mn–Cl distances are remarkably long (2.515, 2.611 Å) for *terminal* ligation at this oxidation level. In $[Mn_4O_3Cl_4(O_2CR)_3(py)_3]$ terminal Mn^{III}–Cl distances are a more reasonable 2.24 Å (average).[23] Thus, the Jahn–Teller distortion takes the form of an elongation along the Cl(3)–Mn(1)–O(5) and Cl(4)–Mn(2)–O(11) axes. In $Mn^{III}(TPP)(py)Cl$, a similar Jahn–Teller elongation leads to a Mn–Cl distance of 2.467(1) Å.[24] The even longer distances in **1** are probably due to the hydrogen bonding with the solvate water molecules (*vide infra*) but, since both Cl(3) and Cl(4) are involved in these additional interactions, it is surprising that there is a 0.1 Å difference between Mn(1)–Cl(3) and Mn(2)–Cl(4).

For complex **5**, unlike complex **1**, the molecule lies on a crystallographically-imposed 2-fold axis passing through O(23), but otherwise the two structures are extremely similar, except that the terminal Cl^- atoms have been replaced by two N_3^- groups. The Mn···Mn separation is 3.153(4) Å, identical to that in **1**. The N(24)–Mn(1)–Mn(1)′–N(24)′ torsional angle is 108.2°. Jahn–Teller elongation, along the N(24)–Mn(1)–O(14) axis, is again evident, and, in particular, the Mn(1)–N(24) distance (2.122(9) Å) is long and comparable to the axially-elongated Mn–N_3^- distance (2.170(6) Å) in $Mn(TACN)(N_3)_3$;[25] the equatorial Mn–N_3^- distances in the latter complex are noticeably shorter (1.911(6) and 1.951(6) Å). There is also a slight, but almost statistically insignificant, difference between the two Mn–N(bpy) distances, suggesting, at most, only a small *trans* influence by the short Mn–O(23) linkage; in complex **1**, the difference is so small as to be insignificant.

For the cation of complex **7**, the structure is very similar to those of **1** and **5**. The Mn···Mn separation is 3.152(2) Å, and the O(8)–Mn(1)–Mn(2)–O(11) torsional angles is 94.4°. Again, the monodentate terminal ligands, in this case H_2O, lie on Jahn–Teller elongation axes, and there is an insignificant *trans* influence of the bridging oxide O(5) on the Mn–N(bpy) lengths.

Overall, it is clear that the three structures are very similar, as emphasized in Table II, and that the identity of the terminal monodentate ligand (Cl^-, N_3^-, and H_2O) has an almost insignificant structural effect. However, as will be described below, there is a more noticeable and rather interesting influence of these ligands on the magnetic properties of the complexes (*vide infra*).

The presence of solvent molecules leads to extensive hydrogen-bonding interactions in the lattices of **1**, **5**·MeCN·$4H_2O$, and **7**. For complex **1**, each water molecule links two Mn_2 molecules by hydrogen bonding to Cl(3) of one molecule and Cl(4) of an adjacent molecule. The O(42)···Cl(3) and O(42)···Cl(4) distances are 3.128 and 3.101 Å, respectively. These interactions are then repeated, leading to one-dimensional polymeric chains. The acetic acid molecule is also hydrogen bonding to the water *via* its OH function (O(42)···O(38) = 2.648 Å) and is not linked to the Mn_2 molecule. For complex **5**·MeCN·$4H_2O$, one of the H_2O molecules links the Mn_2 molecules in a similar fashion as for **1**, forming connecting hydrogen bonds to N(24) and N(24)′ of two adjacent molecules leading to one-dimensional polymers in the lattice; the O(27)···N(24) distance is 2.87 Å. The remaining H_2O and MeCN solvate molecules are not linked to the Mn_2 chains but are themselves hydrogen bonded *via* HO–H···NCMe interactions (O(28)···N(31) = 2.656 Å).

There are now eight structurally-characterized examples of complexes containing the $[Mn_2O(O_2CR)_2]^{2+}$ bridging unit *viz* **1**, **5**, **7** (and the PF_6^- salt),[12] $[Mn_2O(OAc)_2(HB(pz)_3)_2]$ (**9**, $HB(pz)_3^-$ = hydridotris(1-pyrazolyl)borate),[7] $[Mn_2O(OAc)_2(TACN)_2]^{2+}$ (**10**, TACN = 1,4,7-triazacyclononane), $[Mn_2O(OAc)_2(Me_3TACN)_2]^{2+}$ (**11**, Me_3TACN = 1,4,7-trimethyl-1,4,7-triazacyclononane),[8,20,26] $[Mn_2O(OAc)_2(TMIP)_2](ClO_4)_2$ (**12**, TMIP = tris(*N*-methylimidazol-2-yl)phosphine),[27] and $[Mn_2O(OAc)_2(H_2O)(S_2O_8)(bpy)_2]$ (**13**).[22] Complex **9** has been characterized as both the mono- and tetrakis-MeCN solvate. Pertinent structural parameters for the bridging unit of these complexes are collected in Table III. It is evident that there are no major differences between these complexes. The replacement of tridentate $HB(pz)_3^-$, TACN, or TMIP with a bidentate bpy and monodentate Cl^-, N_3^-, or H_2O thus has no serious effect on the bridging unit. A comparison of the structural parameters of **9** and **10** and their Fe^{III} analogues has been provided elsewhere.[7]

Electrochemistry. The electrochemical properties of complexes **1**, **2**, **3**, and **5** have been examined by cyclic voltammetry (CV) in DMF; the choice of the solvent was unfortunately dictated by low solubility of these complexes in other solvents. Complex **1** displays a quasi-reversible oxidation at $E_{1/2}$ = 0.38 V *vs* ferrocene with ΔE_p = 210 mV at 50 mV/s; the reversible ferrocene couple has ΔE_p = 100–120 mV under the same conditions. We suspect DMF/Cl^- exchange equilibria to be occurring in this solvent, which may account for the broadened features. Complexes **2** and **3** show a similar process at $E_{1/2}$ = 0.41 and 0.40 V, respectively. These features are assigned to the $Mn_2^{III}/Mn^{III}Mn^{IV}$ couple. This is analogous to behavior already established for other $[Mn_2O(O_2CR)_2]^{2+}$ species which, however, give better-looking cyclic voltammograms;[7,8,20] further, the one-electron oxidized form of complex **11** has been isolated and structurally characterized,

(22) Blackman, A. G.; Huffman, J. C.; Lobkovsky, E. B.; Christou, G. *J. Chem. Soc., Chem. Commun.* **1991**, 989.
(23) Hendrickson, D. N.; Christou, G.; Schmitt, E. A.; Libby, E.; Bashkin, J. S.; Wang, S.; Tsai, H.-L.; Vincent, J. B.; Boyd, P. D. W.; Huffman, J. C.; Folting, K.; Li, Q.; Streib, W. E. *J. Am. Chem. Soc.* **1992**, *114*, 2455.
(24) Kirner, J. F.; Scheidt, W. R. *Inorg. Chem.* **1975**, *14*, 2081.
(25) Wieghardt, K.; Bossek, U.; Nuber, B.; Weiss, J. *Inorg. Chim. Acta* **1987**, *126*, 39.
(26) Bossek, U.; Wieghardt, K.; Nuber, B.; Weiss, J. *Inorg. Chim. Acta* **1989**, *165*, 123.
(27) Wu, F.-J.; Kurtz, D. M., Jr.; Hagen, K. S.; Nyman, P. D.; Debrunner, P. G.; Vankai, V. A. *Inorg. Chem.* **1990**, *29*, 5174.

confirming its $Mn^{III}Mn^{IV}$ formulation.[28] Complex **5** displays an analogous quasi-reversible oxidation at 0.18 V and an irreversible feature at 0.51 V; the latter is similar to that of NEt_4N_3 (0.43 V) under comparable conditions and is thus assigned to N_3^- oxidation. Complexes **1**, **2**, **3**, and **5** also show additional oxidation features at higher potentials, but these are not well resolved and/or irreversible. Overall, the effect of N_3^- *vs* Cl^- is to shift the oxidation potential to less positive values by about 0.2 V. On the reduction side, all complexes show only broad irreversible features in the −0.50 to −1.0 V range.

Magnetic Susceptibility Studies. The variable-temperature solid-state magnetic susceptibilities of $[Mn_2O(OAc)_2Cl_2(bpy)_2]$ (**1**) and $[Mn_2O(O_2CPh)_2(N_3)_2(bpy)_2]$ (**5**) were measured in the temperature range 5.0 to *ca.* 330 K. Similar studies on the PF_6^- salt of the cation of **7** have already been reported elsewhere.[12] The effective magnetic moment μ_{eff} per Mn_2^{III} for complex **1** decreases gradually with decreasing temperature from 6.33 μ_B at 327.7 K to 5.85 μ_B at 100 K and then more steeply to 2.09 μ_B at 5.0 K (Figure 2). The effective magnetic moment of complex **5**, on the other hand, increases steadily from a value of 6.96 μ_B at 320 K to a maximum of 8.12 μ_B at 30 K and then decreases to 7.45 μ_B at 5.0 K (Figure 3). The magnetic behavior of **1** is that expected for a pair of antiferromagnetically-coupled high-spin ($S = 2$) Mn^{III} ions, while that observed for **5** is characteristic of a net ferromagnetic interaction between the two Mn^{III} ions. The behavior of μ_{eff} at low temperature for **5** is similar to that observed in ferromagnetically-coupled dinuclear Ni^{II} complexes.[29] The increasing moment is due to population of the $S = 4$ ground state, while the decrease in moment at lower temperatures is due to changes in the populations of the components of the $S = 4$ ground-state multiplet that are split by contributions from zero-field splitting and Zeeman interactions.

A model was constructed to analyze the magnetic data of **1** and **5** that included in the Hamiltonian for the dinuclear complex the isotropic Heisenberg exchange interaction $-2J\hat{S}_1\cdot\hat{S}_2$, an isotropic Zeeman interaction and the axial zero-field splitting terms, $D(\hat{S}_{iz}^2) - S_i(S_i + 1)/3$ ($i = 1,2$), for both ions. The Hamiltonian matrix was constructed with a set of uncoupled product basis functions using the program PAIR.[30] The eigenvalues and eigenvectors of the system are evaluated by diagonalization of the 25 × 25 Hamiltonian matrix including the Zeeman terms. The paramagnetic susceptibility χ of a dinuclear Mn^{III} complex was then obtained from the calculated magnetization using eq 5,[31] where the derivatives of the energy of each level with

$$M = \chi H = N\sum_{i=1}^{P}\left(\frac{-\delta E_i}{\delta H}\right)\exp(-E_i/kT)/\sum_{i=1}^{P}\exp(-E_i/kT) \quad (5)$$

respect to the magnetic field ($\delta E_i/\delta H$) were calculated from the appropriate eigenvector using the Hellman–Feynman theorem.[32] The whole calculational procedure was incorporated into a nonlinear least-squares fitting computer program[17] and used to fit the temperature dependence of the magnetic moments of **1** and **5** as a function of J (the exchange coupling parameter), D (the single-ion zero-field splitting), and an isotropic g value.

For complex **1**, it was found that a good fit of the μ_{eff} *vs* temperature data could be obtained, except at the lowest temperatures where the theoretical values of μ_{eff} were found to be smaller than those observed. In the case of antiferromagnetically-coupled complexes, it is frequently the presence of a small amount of paramagnetic impurity that causes this deviation. Thus, in the fitting of the data for complex **1**, we included a susceptibility term (Curie law behavior) for a paramagnetic $S = 2$ impurity. The solid line in Figure 2 illustrates how good this fit is; the fitting parameters are $g = 1.88$, $J = -4.1$ cm^{-1}, and $D_1 = D_2 = -0.07$ cm^{-1} with 0.8% by weight of a paramagnetic $S = 2$ impurity. It should be emphasized that the value of J is not appreciably influenced by the amount of paramagnetic impurity. On the other hand, it is our experience that the fitting of μ_{eff} *vs* temperature data is not very sensitive to the single-ion zero-field splitting parameter D.

Least-squares fitting of the μ_{eff} *vs* temperature data for complex **5** with the matrix diagonalization approach outlined above gave $g = 1.86$, $J = +8.8$ cm^{-1}, and $D_1 = D_2 = 0.3$ cm^{-1}. The solid line in Figure 3 represents this fit. It can be seen that there is some deviation between the line that represents the best fit and the experimental data, particularly in the low-temperature region. Data were collected for several samples of complex **5** and were

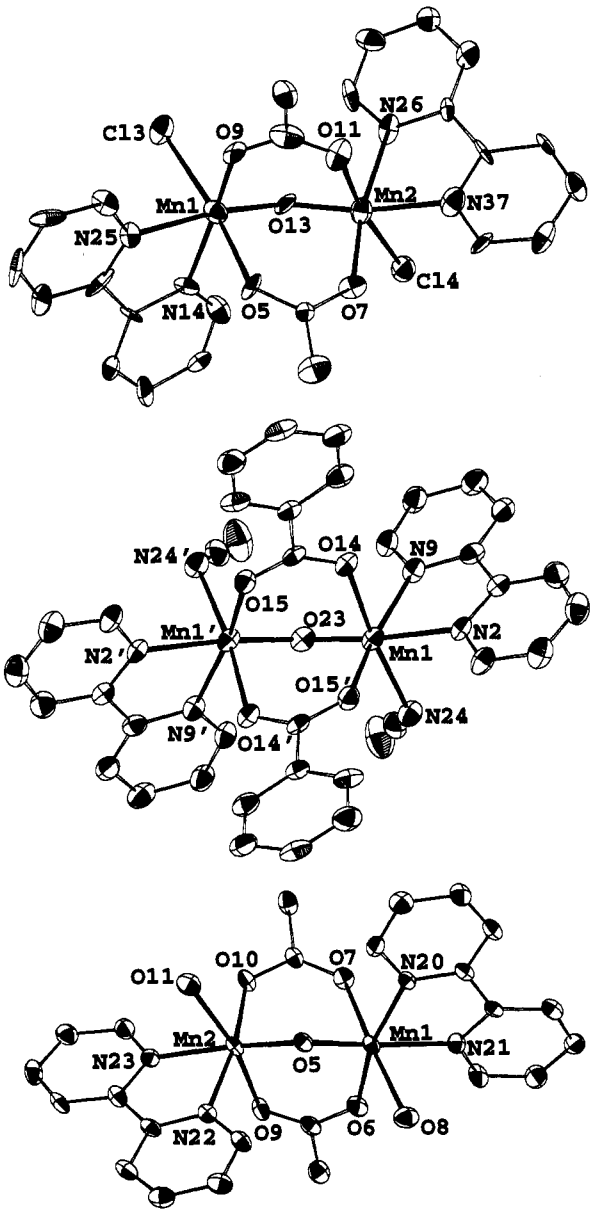

Figure 1. ORTEP representations of complexes **1** (top), **5** (middle), and the anion of **7** (bottom) at the 50% probability level; bpy C atoms are numbered sequentially from one N atom to the other.

(28) Weighardt, K.; Bossek, U.; Bonvoisin, J.; Beauvillain, P.; Girerd, J.-J.; Nuber, B.; Weiss, J.; Heinze, J. *Angew. Chem., Int. Ed. Engl.* **1986**, *25*, 1030.

(29) Ginsberg, A. P.; Sherwood, R. C.; Brookes, R. W.; Martin, R. L. *J. Am. Chem. Soc.* **1971**, *93*, 5927.

(30) Schmitt, E. A.; Hendrickson, D. N., unpublished results.

(31) Vermaas, A.; Goeneveld, W. L. *Chem. Phys. Lett.* **1974**, *27*, 583.

(32) (a) Boyd, P. D. W.; Martin, R. L. *J. Chem. Soc., Dalton Trans.* **1979**, 92. (b) Gerloch, M.; McMeeking, R. F. *J. Chem. Soc., Dalton Trans.* **1975**, 2443.

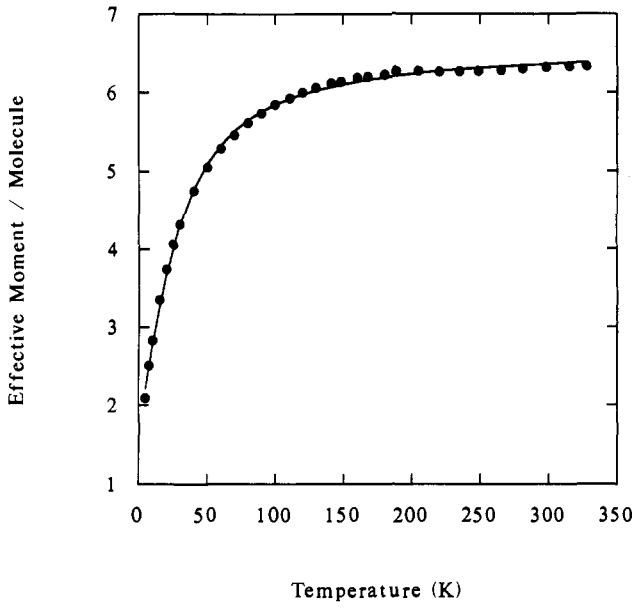

Figure 2. Plot of effective magnetic moment per molecule *versus* temperature for $[Mn_2O(OAc)_2Cl_2(bpy)_2]\cdot AcOH\cdot H_2O$ (**1**) at 10.0 kG. The solid line represents a least-squares fit of the data.

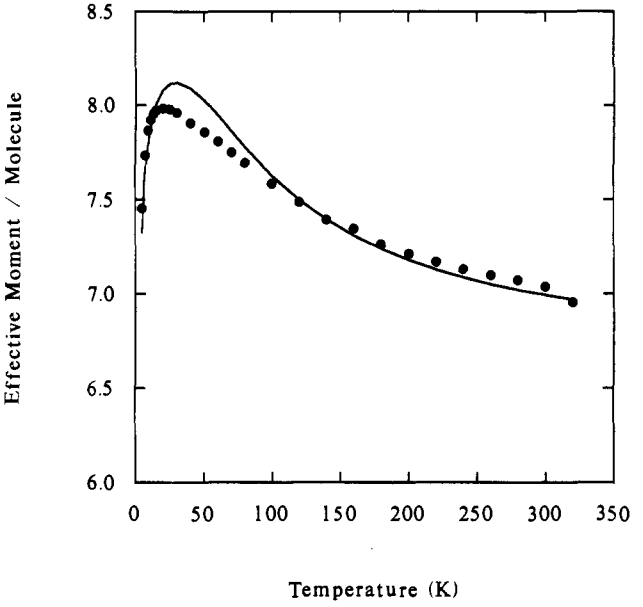

Figure 3. Plot of effective magnetic moment per molecule *versus* temperature for $[Mn_2O(O_2CPh)_2(N_3)_2(bpy)_2]\cdot MeCN\cdot 3/2H_2O$ (**5**) at 10.0 kG. The solid line represents a least-squares fit of the data.

found to be reproducible. The sample was restrained in parafilm, so the deviation at low temperatures cannot be attributed to torquing of small crystallites in a magnetic field. An examination of the packing arrangement for complex $5\cdot MeCN\cdot 4H_2O$ shows that the dimeric complexes are joined in an infinite chain by hydrogen bonds between the coordinated azide ligands and H_2O molecules present in the lattice. Weak intermolecular exchange interactions propagated by the hydrogen-bonding network are the likely origin of the deviation between the solid line and the experimental data in Figure 3. A figure showing the hydrogen-bonding network is available in supplementary material.

Field-Dependent Magnetization of $[Mn_2O(OAc)_2(N_3)_2(bpy)_2]$ (5). The net ferromagnetic interaction between the two Mn^{III} ions in **5** gives a $S = 4$ ground state separated from the lowest energy excited state, which has $S = 3$, by $|8J| = 70.4$ cm^{-1}. Measurements of the magnetic field dependence of the magnetization of a polycrystalline sample of **5** were carried out at fields

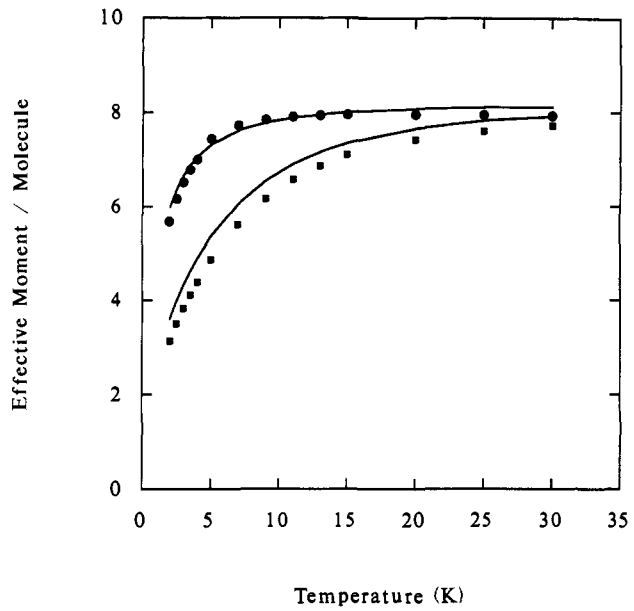

Figure 4. Plot of effective magnetic moment at 10.0 kG (upper) and 50.0 kG (lower) *versus* temperature for $[Mn_2O(O_2CPh)_2(N_3)_2(bpy)_2]\cdot MeCN\cdot 3/2H_2O$ (**5**). Both data sets were simultaneously least-squares fit to give the two solid lines by a full matrix diagonalization method.

of 10.0 and 50.0 kG in the range of 2.0–30.0 K to characterize further the ground state of this complex. Figure 4 shows a plot effective magnetic moment *versus* temperature for the data collected at either 10.0 or 50.0 kG field. It can be seen that increasing the magnetic field from 10.0 to 50.0 kG leads to a greater effect for the Zeeman interaction. The value of μ_{eff} is reduced owing to saturation effects.

The 10.0 and 50.0 kG low-temperature μ_{eff} data observed for complex **5** were simultaneously least-squares fit to the matrix diagonalization model described above for fitting the full temperature dependence of the susceptibility data measured at 10 kG. The two solid lines in Figure 4 result from such a least-squares fit, which gives the parameters $g = 1.86$, $J = +8.8$ cm^{-1}, and $D_1 = D_2 = 0.3$ cm^{-1}. The fit is reasonable in view of the above-mentioned possible intermolecular interactions. Clearly, complex **5** has an $S = 4$ ground state.

A value of $D = 0.3$ cm^{-1} for the axial zero-field splitting in the $S = 4$ ground state of complex **5** is probably in the range expected for a Mn^{III}_2 complex. Of course, the magnitude of D for the $S = 4$ state reflects the magnitude of the axial *single-ion* zero-field interaction parameters at each Mn^{III} ion. A Mn^{III} ion in a tetragonally-elongated coordination site with C_{4v} symmetry will have a $^5B_1$ ($e^2b_2^1a_1^1$) ground state with $^5A_1$ ($e^2b_2^1b_1^1$), $^5B_2$ ($e^2a_1^1b_1^1$), and ^5E ($e^1b_2^1a_1^1b_1^1$) excited states. The ^5E and $^5B_2$ excited states can interact with the $^5B_1$ ground state to give a zero-field splitting of the $^5B_1$ state into levels with $M_s = 0$, ± 1, and ± 2. When $D < 0$, the $M_s = \pm 2$ level is at the lowest energy, whereas when $D > 0$, then the $M_s = 0$ level is at the lowest energy. Depending on the magnitudes of distortion and crystal field interactions, triplet states can also be involved in a spin-orbit interaction with the $^5B_1$ ground state. D values for Schiff-base and porphyrin complexes of Mn^{III} have been found[33] to fall in the range of -1.0 to -3.0 cm^{-1}.

Magnetostructural Commentary. The magnitude of the magnetic exchange interactions between the two Mn^{III} ions found in complexes **1** and **5** may be compared with those reported for the other Mn_2^{III} complexes that have the $[Mn_2O(O_2CR)_2]^{2+}$ bridging unit. As summarized in Table III, the Mn_2^{III} ions are antifer-

(33) (a) Kennedy, B. J.; Murray, K. S. *Inorg. Chem.* **1985**, *24*, 1552 and 1557. (b) Mathe, J.; Schinkel, C. J.; VanAnsted, W. A. *Chem. Phys. Lett.* **1975**, *33*. 528. (c) Behere, D. V.; Marathe, V. R.; Mitra, S. *Chem. Phys. Lett.* **1981**, *81*, 57. (d) Behere, D. V.; Mitra, S. *Inorg. Chem.* **1980**, *19*, 992.

Table II. Comparison of Structural Parameters for **1**, **5**, and the Anion of **7**

parameter[a]	1	5	7
Mn···Mn	3.153(3)	3.153(4)	3.152(2)
Mn–O_b	1.788(11)	1.802(4)	1.793(4)
	1.777(12)		1.800(4)
Mn–X	2.515(6)	2.122(9)	2.269(4)
	2.611(6)		2.302(4)
Mn–O_c[b]	2.214(12)	2.131(7)	2.175(4)
	2.196(13)		2.164(4)
Mn–O_c[c]	1.955(13)	2.043(7)	1.939(4)
	1.934(13)		1.946(4)
Mn–N_t	2.087(13)	2.092(8)	2.082(4)
	2.084(16)		2.073(4)
Mn–N_c	2.062(15)	2.142(8)	2.070(4)
	2.071(16)		2.060(4)
Mn–O_b–Mn	124.3(7)	122.0(5)	122.7(2)
X–Mn–O_c[b]	173.0(3)	172.4(3)	168.3(1)
	171.6(4)		175.8(1)
X–Mn–O_c[c]	93.0(4)	91.7(3)	89.2(2)
	93.8(4)		87.2(2)
O_b–Mn–O_c[b]	95.1(5)	95.4(2)	97.2(2)
	93.5(5)		91.7(2)
O_b–Mn–O_c[c]	98.8(5)	99.8(3)	101.6(2)
	100.5(6)		97.2(2)
O_c–Mn–O_c	86.9(5)	87.0(3)	91.2(2)
	90.4(5)		91.9(2)

[a] O_b = bridging oxide, O_c = bridging carboxylate, N_t = N *trans* to O_b, N_c = N *cis* to O_b. [b] *Trans* to X. [c] *Trans* to N.

Table III. Exchange Interactions[a] and Selected Structural Parameters for $[Mn_2O(O_2CR)_2]^{2+}$ Complexes

complex	Mn···Mn, Å	Mn–O, Å	Mn–O–Mn, deg	J, cm^{-1}	ref
1	3.153(3)	1.788(11)	124.3(7)	–4.1	*b*
		1.777(12)			
5	3.153(4)	1.802(4)	122.0(5)	+8.8	*b*
7[c]	3.132	1.781(5)	122.9	–3.4	12
		1.784(5)			
9	3.159(1)[d]	1.780(2)[d]	125.1(1)[d]	*ca.* –0.5[f]	7
	3.175(1)[e]	1.790(3)[e]	125.0(3)[e]		
10	3.084(3)	1.80(1)	117.9(2)		8
11	na	1.810(4)	120.9(1)	+9	20
12	3.164(5)	1.797(11)	124.4(6)	*ca.* –0.5[g]	27
		1.781(11)			
13	3.145(5)	1.735(10)	125.1(6)	na	22
		1.810(10)			

[a] Values using the $-2JS_1 \cdot S_2$ convention. [b] This work. [c] PF_6^- salt, all data from ref 12. [d] 4MeCN solvate. [e] MeCN solvate. [f] Quoted range –0.2 to –0.7 cm^{-1} for both solvate forms. [g] Similar to **9**; na = not available.

romagnetically coupled in **1**, the PF_6^- version of **7**, $[Mn_2O(OAc)_2(HB(pz)_3)_2]$ (**9**), and $[Mn_2O(OAc)_2(TMIP)_2](ClO_4)_2$ (**12**) and ferromagnetically coupled in **5** and $[Mn_2O(OAc)_2(Me_3TACN)_2]$ (**11**).

In Table III are compared the structural parameters of the oxide-bridged core, *viz.* the Mn···Mn distance, and the Mn–O distances and Mn–O–Mn angles. It is clear that the Mn···Mn separation is not a factor in determining the precise value of J, complexes **1** and **5** having identical values but different signs of J. It should be emphasized that for all $[Mn_2O(OAc)_2]^{2+}$ species, the exchange interactions are extremely weak. Further, the J values only span a range of ~13 cm^{-1}. Since the exchange interaction in a d^4–d^4 dimer will be the net sum of various antiferromagnetic and ferromagnetic contributions, it is not anticipated that a correlation of J with a single structural parameter will exist. The overall weak couplings have been rationalized at a qualitative level by consideration of the symmetry of the pairwise overlaps of the magnetic orbitals; this has also provided a useful guide to the variation of J with M^{3+} (and d^n) across the first transition series.[34] In the present case, we have sought to identify the subtle structural differences between **5**/**11** and the other complexes that result in the former pair being ferromagnetically coupled. However, no clear-cut trends are obvious. The Mn–O–Mn angles and Mn–O lengths in **5** and **11** are *very* slightly smaller and greater, respectively, than for complexes with negative J values. However, applying strictly the statistical 3σ criterion for esds makes all these values insignificantly different.

Since peripheral ligands are also varying, further discussion is restricted to the subset of complexes **1**, **5**, and **7**, varying only in one ligand per Mn. These complexes have J values spanning a range of ~13 cm^{-1}, and one might normally be tempted to conclude that, within experimental variation, the complexes are essentially indistinguishable magnetochemically. But, of course, a distinct difference does indeed exist between them in that **5** is ferromagnetically coupled, whereas **1** and **7** are antiferromagnetically coupled; this difference is real and cannot be ignored as due to experimental variation. Thus, we feel duty-bound to attempt a rationalization of the differences between **5** and **1**/**7** based on the structures of the three complexes. As described above and in Table III, the three structures are essentially superimposable *except* for the terminal monodentate ligands (N_3^-, Cl^-, or H_2O). As is customary in discussing oxide-bridged dimers, each z axis is placed along the Mn–O bond (see below). The

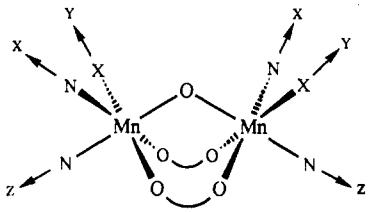

short Mn–O bond and Jahn–Teller elongation lead to empty d_{z^2} and singly-occupied $d_{x^2-y^2}$ orbitals. We can now tentatively suggest the following rationalization for the variation of J with terminal ligand X. For X = Cl^- or H_2O, these weak field ligands have relatively long Mn–X bond distances (2.515/2.611 and 2.269/2.302 Å, respectively) which, when combined with their relatively poor π-donor abilities, will result in small (relative to N_3^-) influence on the $d_{x^2-y^2}$ and d_π metal orbitals. In contrast, for stronger field N_3^-, the Mn–N_3^- bond in **5** is significantly shorter (2.122 Å), and this would result in a greater influence on the $d_{x^2-y^2}$ and d_π metal orbitals. It is expected that the σ influence of the N_3^- ligand will be greater than its π influence. The d_π orbitals contribute to both ferromagnetic and antiferromagnetic exchange interactions *via* the bridging oxide p_π orbitals,[34] whereas the $d_{x^2-y^2}$ orbitals can contribute antiferromagnetically *via* a pathway involving the bridging carboxylates. In both cases, the N_3^- ligands will raise the energy of the metal magnetic orbitals, increasing the energy gap between them and those of the bridging ligands. The effect is thus to weaken slightly the ferromagnetic and antiferromagnetic exchange interactions *via* the O p_π pathway and the antiferromagnetic interaction *via* the carboxylates. Since the σ effect of the N_3^- should dominate, this qualitatively rationalizes an overall slight decrease in the net antiferromagnetic contributions to the J value and a consequent slight shift to a more positive value. We emphasize that these effects would be expected to be very small and normally inconsequential, especially when, as in the corresponding $[Fe_2O(O_2CR)_2]^{2+}$ complexes, the d_{z^2} orbitals are singly-occupied and a strong antiferromagnetic d_{z^2}/d_{z^2} interaction[34] *via* the bridging O p orbitals dominates by far and leads to a large overall negative J value. However, for the present $[Mn_2O]^{4+}$ complexes where the overall J values are close to zero, the described effects can serve to yield a noticeable difference in that the ferromagnetic contributions in **5** slightly dominate overall and give a net positive J value.

(34) Hotzelmann, R.; Wieghardt, K.; Florke, U.; Haupt, H.-J.; Weatherburn, D. C.; Bonvoisin, J.; Blondin, G.; Girerd, J.-J. *J. Am. Chem. Soc.* **1992**, *114*, 1681.

Discussion and Biological Relevance

Synthetic procedures have been devised that allow convenient access routes to dinuclear complexes containing the $[Mn_2O(O_2CR)_2]^{2+}$ bridging unit and terminal bpy groups. A sixth coordination site is thus available at each Mn for binding additional monodentate groups, and the preparation of the Cl^-, N_3^-, and H_2O complexes is readily accomplished. Employment of tridentate capping ligands is thus clearly not a prerequisite for stabilizing the $[Mn_2O(O_2CR)_2]^{2+}$ core, although complexes with tridentate ligands do seem more robust with respect to redox changes, as evidenced by their more ideal and reversible electrochemical behavior when studied by cyclic voltammetry. Structurally, the several crystallographically-characterized complexes are essentially superimposable, except for the identity of their peripheral ligands.

If, as is currently thought, the dinuclear site of Mn catalase (and, possibly, also Mn ribonucleotide reductase) involves a similar $[Mn_2O(O_2CR)_2]^{2+}$ core,[2,4] it is likely that substrate binding sites in peripheral positions will also be present. This would be as already established for the related Fe_2 biomolecules, hemerythrin (Hr),[4] and Fe ribonucleotide reductase.[35] In addition, again as for hemerythrin, further study of Mn catalase may possibly lead to the preparation of various substrate–analog-bound forms *viz.* Cl^-, N_3^-, aquo-catalase (which may be the resting form of the enzyme), and possibly others, containing the indicated exogenous terminal ligands. Indeed, we note that both Cl^- and N_3^- are reported to be inhibitors of Mn catalase.[2] Although N_3^- only weakly inhibits the *T–album* enzyme,[36a] it is a more potent inhibitor of the *T. thermophilus* catalase.[36b] More recently, the *L. plantarum* enzyme is also reported to be inhibited by azide.[2] The conclusion from these studies is that N_3^- binds to the Mn. Similar conclusions were reached from parallel studies employing SCN^- and F^-, and it therefore appears that a variety of exogenous ligands are capable for ligating to the Mn.[2] Thus, the series **1**, **5**, and **7** may prove of some utility in the future as models for some of these various enzyme forms.

With the above in mind, we have felt it particularly important to characterize **1** and **5** by magnetic susceptibility studies to complement data already available for the PF_6^- version of **7**. As might have been expected, the $Cl^-/N_3^-/H_2O$ variation has very little effect on the overall exchange interaction between the Mn^{III} sites, giving values spanning a range of only 13 cm^{-1}. However, since the exchange interactions are very weak (ca. zero), this range is sufficient to have an apparently large effect in leading to a ferromagnetic interaction in complex **5** and a $S = 4$ ground state, in contrast to antiferromagnetically-coupled **1** and **7** and their $S = 0$ ground states. It is proposed that the sensitivity of the exchange interaction to the monodentate terminal ligands is due to exchange pathways involving the d_π orbitals with the oxide and the $d_{x^2-y^2}$ orbitals with the bridging carboxylate groups. Since substrate–analogue forms of the catalase, should they become accessible, will have identical ligation sets except for the exogenous ligands, it will be interesting to see whether similar variations in the *sign* of J will be encountered.

It should be mentioned that the most extensive set of complexes containing the $[M_2(\mu\text{-}O)(\mu\text{-}O_2CR)_2]$ core for which magnetochemical data are available is for $M = Fe^{III}$.[4,37] In these cases, the d_{z^2} orbitals are half-occupied and an antiferromagnetic d_{z^2}/d_{z^2} exchange interaction mediated by the bridging oxide ion dominates and leads to overall antiferromagnetic interactions with $-J$ in the *ca.* 108–132-cm^{-1} range. No simple conclusion can be drawn concerning the variation within the latter range as a function of peripheral ligands owing to too many structural and ligand differences. However, the various forms of the protein met-X-Hr ($X = N_3^-$, Cl^-, etc.) differ only in the identity of X and would be attractive for J value comparisons but we are unaware of J values having been obtained yet on these systems. In contrast, for the OH-bridged di*ferrous* forms, the J values are much smaller (deoxy Hr; $-J = 12$–36 cm^{-1}),[4,38,39] and we are very interested to note that deoxy-N_3^-Hr has been reported to have a small but *positive* J value, i.e., it is ferromagnetically coupled.[39] It has been suggested that this is due to the OH^- bridge in deoxy-Hr converting to a H_2O bridge in deoxy-N_3^-Hr; our results for complexes **1**, **5**, and **7** would alternatively suggest that the positive J value may be simply due to the presence of N_3^- and not a change in the identity of the bridge. However, the positive J values for both **5** and deoxy-N_3^-Hr may be merely a coincidence and additional data on $[M_2O(O_2CR)_2]$ and $[M_2(OH)(O_2CR)_2]$ species are required before firmer conclusions can be drawn.

Concluding Comments

It has been shown that a series of complexes can be readily obtained that possess the general formula $[Mn_2O(O_2CR)_2X_2(bpy)_2]$ and thus differ only in the identity of X. The series currently consists of $X = Cl^-$, N_3^-, and H_2O and attempts to extend it to other groups (e.g., F^-, SCN^-, CN^-) by, for example, ligand exchange reactions with **1** are currently in progress. Such complexes are proving invaluable in permitting the influence of X on a variety of properties to be assessed, such as structural and magnetochemical parameters. The ability to document these influences should prove extremely useful as data on the various Mn_2 enzymes becomes increasingly available and the desire to understand their structure/function relationships continues to grow.

Acknowledgment. This work was supported by NIH Grants GM 39083 (to G.C.) and HL 13652 (to D.N.H.).

Supplementary Material Available: Complete listings of atomic coordinates, isotropic and anisotropic thermal parameters, bond lengths and angles, figures showing hydrogen-bonding interactions, and magnetic susceptibility data (24 pages); tables of calculated and observed structure factors (18 pages). Complete copies of the MSC structure reports (87118, 87178, and 90286 for **1**, **5**, and **7**, respectively) are available on request from the Indiana University Chemistry Library. This material is contained in many libraries on microfiche, immediately follows this article in the microfilm version of the journal, and can be ordered from the ACS; see any current masthead page for ordering information.

(35) Nordlund, P.; Sjoberg, B.-M.; Eklund, H. *Nature* **1990**, *345*, 593.
(36) (a) Allgood, G. S.; Perry, J. J. *J. Bacteriol.* **1986**, *168*, 563. (b) Barynin, V. V.; Grebenko, A. I. *Dokl. Akad. Nauk. SSSR* **1986**, *286*, 461.
(37) Gorun, S. M.; Lippard, S. J. *Inorg. Chem.* **1991**, *30*, 1625, and references cited therein.
(38) Maroney, M. J.; Kurtz, D. M., Jr.; Nocek, J. M.; Pearce, L. L.; Que, L., Jr. *J. Am. Chem. Soc.* **1986**, *108*, 6871.
(39) Reem, R. C.; Solomon, E. I. *J. Am. Chem. Soc.* **1987**, *109*, 1216, and **1984**, *106*, 8323.